Global properties of Kaluza-Klein cosmologies

David L. Wiltshire
Department of Applied Mathematics and Theoretical Physics, University of Cambridge, Silver Street, Cambridge CB3 9EW, England
(Received 27 April 1987)

The qualitative theory of dynamical systems is used to present an analysis of the phase space of Kaluza-Klein cosmological solutions with even-dimensional internal space, an arbitrary cosmological constant, and Freund-Rubin compactification. If either the physical or internal manifold has a single spatial dimension the cosmological solutions may correspond to black-hole interiors and pathological behavior can be expected. It is shown that such behavior does not occur in general, however. Some solutions with dilatons are also discussed.

I. INTRODUCTION

It is generally believed that higher dimensions must play an important dynamical role in the very early evolution of the Universe. Ideally some sort of dynamical mechanism should exist to explain (i) why the "physical" dimensions have expanded relative to the extra dimensions so that as yet the radii of curvature of the physical and internal spaces differ by a factor of the order of 10^{61}, and (ii) why the physical space should have three spatial dimensions. Mechanisms are known which incorporate a natural splitting of the physical and internal dimensions. These include the Freund-Rubin mechanism,[1] the Casimir effect associated with matter fields or zero-point gravitational energies,[2] and the effect of higher-derivative terms in the gravitational action.[3] Although such mechanisms may provide some insights with regard to the first of these questions, the second question is still wide open.

A typical approach to Kaluza-Klein cosmology is to set aside the question of the nature of the initial singularity and instead to focus attention on the behavior of the Universe at times when the physical and internal spaces can be treated on a different footing.[4] The d-dimensional metric may then be decomposed as

$$ds^2=dt^2-a^2(t)g_{ij}dx^i dx^j-b^2(t)g_{IJ}dy^I dy^J\ , \qquad (1.1a)$$

where, for example, $g_{ij}(x)$ and $g_{IJ}(y)$ are metrics on Einstein spaces of dimension m and $n=d-m-1$, respectively, so that they are described by Ricci tensors with components

$${}^m R_{ij}=(m-1)k_a\delta_{ij} \qquad (1.1b)$$

and

$${}^n R_{IJ}=(n-1)k_b\delta_{IJ} \qquad (1.1c)$$

in an orthonormal frame. The radii of curvature of the two spaces have been scaled so that $k_a,k_b=-1,0,+1$. (Although there is no observational reason to assume that the internal dimensions expand isotropically, this is a common simplifying assumption.) A large number of models based on the ansatz (1.1) together with various matter degrees of freedom have been studied over the past few years.[5]

To be of physical relevance cosmological solutions must exist for which the internal space is static at late times. A number of such solutions have been found and their stability analyzed. However, little is known in general about the global properties of the spacetimes (1.1). Indeed, in cases where the global properties of the spacetimes are known, in five-dimensional vacuum cosmologies,[6-8] for example, some bizarre behavior takes place. One obtains the result that the physical universe is the interior of a five-dimensional black hole. This can be a very dangerous place to exist. If matter is included in the form of five-dimensional dust, for example, singularities can form even when the scale factor a and the Hubble parameter $\dot{a}/a$ are finite.[6,7]

Naturally one would like to know whether such pathologies are merely a result of the high degree of symmetry of the models, whether they are a dimension-dependent phenomenon, or whether perhaps they are a generic feature of many higher-dimensional models. To answer this question for models more complex than the five-dimensional ones is difficult since exact solutions are not known in general. However, as Belinsky *et al.*[9] have shown, for inflationary models in four dimensions, if the dimension of the phase space of classical solutions is sufficiently small then an analysis of its qualitative properties can yield information about all the relevant global features of the solutions. We shall present such an analysis here for some general models. Our conclusion is that apart from a very small set of solutions in the open ($k_a=-1$) models the behavior discussed above only occurs when the internal space has a single spatial dimension.

We will take the action in d dimensions to have the general form

$$\int\sqrt{g}\left[\frac{-R}{4\kappa^2}-(-1)^n\frac{f(\sigma)}{2n!}F_{\mu_1\cdots\mu_n}F^{\mu_1\cdots\mu_n}+\tfrac{1}{2}g^{\mu\nu}\partial_\mu\sigma\partial_\nu\sigma-V(\sigma)\right], \qquad (1.2a)$$

where

$$F_{\mu_1\mu_2\cdots\mu_n}=n\partial_{[\mu_1}A_{\mu_2\cdots\mu_n]} \qquad (1.2b)$$

is the field strength associated with an Abelian gauge field $A_{\mu_1\cdots\mu_{n-1}}$, $\kappa^2=4\pi G$, $g\equiv|\det g_{\mu\nu}|$, and f and V are as yet unspecified functions of the real scalar field σ. Since we are interested in homogeneous solutions we shall assume that $\sigma=\sigma(t)$ throughout. In all cases we will take $F_{\mu_1\cdots\mu_n}$ to be given by the Freund-Rubin ansatz,[11] so that

$$F=\frac{q}{b^n}dy^1\wedge dy^2\wedge\cdots\wedge dy^n\ . \tag{1.3}$$

This automatically satisfies the Maxwell-type equation derived from the variation of (1.2). The remaining field equations to be solved are

$$m\frac{\ddot a}{a}+n\frac{\ddot b}{b}=\frac{4\kappa^2V}{d-2}-\frac{2\kappa^2(n-1)fq^2}{(d-2)b^{2n}}-2\kappa^2\dot\sigma^2\ , \tag{1.4a}$$

$$\frac{\ddot a}{a}+n\frac{\dot a\dot b}{ab}+(m-1)\frac{1}{a^2}(\dot a^2+k_a)=\frac{4\kappa^2V}{d-2}-\frac{2\kappa^2(n-1)fq^2}{(d-2)b^{2n}}\ , \tag{1.4b}$$

$$\frac{\ddot b}{b}+m\frac{\dot a\dot b}{ab}+(n-1)\frac{1}{b^2}(\dot b^2+k_b)=\frac{4\kappa^2V}{d-2}+\frac{2\kappa^2mfq^2}{(d-2)b^{2n}}\ , \tag{1.4c}$$

$$\ddot\sigma+\dot\sigma\left[m\frac{\dot a}{a}+n\frac{\dot b}{b}\right]=-V'-\frac{f'q^2}{2b^{2n}}\ , \tag{1.4d}$$

where an overdot denotes d/dt and a prime $d/d\sigma$.

To study Eqs. (1.4) using the qualitative theory of dynamical systems it is convenient to rewrite them as the system of first-order differential equations

$$\dot a=Ha\ , \tag{1.5a}$$

$$\dot b=Ib\ , \tag{1.5b}$$

$$\sqrt{2}\kappa\dot\sigma=K\ , \tag{1.5c}$$

$$\dot H=\frac{4\kappa^2V}{d-2}-mH^2-nHI-(m-1)\frac{k_a}{a^2}-\frac{2(n-1)f\kappa^2q^2}{(d-2)b^{2n}}\ , \tag{1.5d}$$

$$\dot I=\frac{4\kappa^2V}{d-2}-mHI-nI^2-(n-1)\frac{k_b}{b^2}+\frac{2mf\kappa^2q^2}{(d-2)b^{2n}}\ , \tag{1.5e}$$

$$\dot K=-(mH+nI)K-\sqrt{2}\kappa\left[V'+\frac{f'q^2}{2b^{2n}}\right]\ , \tag{1.5f}$$

subject to the constraint

$$\frac{2\kappa^2q^2}{b^{2n}}+4\kappa^2V+K^2-m(m-1)\left[H^2+\frac{k_a}{a^2}\right]-2mnHI-n(n-1)\left[I^2+\frac{k_b}{b^2}\right]=0\ , \tag{1.5g}$$

Equations (1.5a)–(1.5c) are definitions for the physical and internal-space Hubble parameters H and I, and the quantity K. In general, Eqs. (1.5) are of course a very complex system. However, in most of this paper we shall consider the particular case in which the dilation $\sigma(t)$ is set identically to zero, $f=1$, and $2\kappa^2V=\Lambda$ is a d-dimensional cosmological constant. In Sec. II we will discuss those solutions which correspond to black-hole interiors. In Secs. III and IV we will consider the general solutions with n even. In Sec. V some solutions with nontrivial dilatons are discussed. Some concluding remarks are given in Sec. VI.

II. THE REDUCTION TO TWO DIMENSIONS

The behavior of the solutions discussed by Matzner and Mezzacappa[6,7] and Gibbons and Townsend[8] seems to be a generic feature at least of models in which one of the two spaces has only one spatial dimension. To see this we will consider the case $m=1$, although equivalently, we could take the perhaps more physically relevant case $n=1$ and replace the "magnetic compactification" ansatz (1.3) with the "electric compactification" ansatz

$$F=\frac{qa}{b^2}dt\wedge dy\ , \tag{2.1}$$

where y is now the single internal dimension and F is a two-form.

Equations (1.4) with $m=1$, $f=1$, $2\kappa^2V=\Lambda$, and $\sigma\equiv0$ are easily integrated[10] and the solutions are $a^2=\dot b^2=\Delta$, where

$$\Delta=\frac{2GM}{b^{d-3}}-\frac{2\kappa^2q^2}{(d-2)(d-3)b^{2(d-3)}}+\frac{2\Lambda b^2}{(d-1)(d-2)}-k_b\ . \tag{2.2}$$

We may use b as a time coordinate to write the metric in the form

$$ds^2=\frac{db^2}{\Delta}-\Delta dx^2-b^2g_{IJ}dy^Idy^J\ . \tag{2.3}$$

Reality of $a\equiv\dot b$ requires $\Delta>0$. However, the $\Delta=0$ surface is only a coordinate singularity and the global structure of the solution is obtained by extending to values $\Delta<0$. If $k_b=1$, for example, and the internal space is taken to be S^{d-2} then the global structure of the spacetime is that of the Reissner-Nordström–de Sitter solution in arbitrary dimensions, as obtained by Tangherlini.[11]

The spacetimes may be classified according to the structure of their horizons and singularities. We will restrict our attention to the case in which d is even and $q\neq0$. There are then essentially nine distinct cases of spacetimes with regions corresponding to cosmological solutions. Degenerate cases occur when $\Delta=d\Delta/db=0$, i.e., when $b=b_\pm$, where

$$b_{\pm}^{-(d-3)}=\frac{1}{4\kappa^2 q^2}\{(d-1)(d-3)GM \pm\epsilon[(d-1)^2(d-3)^2G^2M^2 -8(d-3)k_b\kappa^2q^2]^{1/2}\}\ , \tag{2.4}$$

$$\epsilon=\begin{cases}+1, & M\geq 0\ ,\\ -1, & M<0\ .\end{cases}$$

To aid in our classification let us define $q_1{}^2$, $q_2{}^2$, λ_1, and λ_2 by

$$q_1{}^2=\frac{8q^2}{(d-1)^2(d-3)}\ , \tag{2.5a}$$

$$q_2{}^2=\frac{2q^2}{(d-2)(d-3)}\ , \tag{2.5b}$$

$$\lambda_1=\frac{(d-2)(d-3)k_b}{2b_+{}^2}-\frac{\kappa^2q^2}{b_+{}^{2(d-2)}}\ , \tag{2.6a}$$

$$\lambda_2=\frac{(d-2)(d-3)k_b}{2b_-{}^2}-\frac{\kappa^2q^2}{b_-{}^{2(d-2)}}\ . \tag{2.6b}$$

In the definitions (2.6a) and (2.6b), b_+ and b_- are given by (2.4) for each M and q for which (2.4) has real solutions. If d is even, solutions of $\Delta=0$ with $M<0$ may be obtained by setting $b\rightarrow -b$ in the solutions with $M>0$. Thus, we may assume $M\geq 0$ without loss of generality. The global properties of the metric for the nine cases are best summarized by drawing Carter-Penrose diagrams, as in Fig. 1, where each point represents an internal space. Horizons are represented by straight lines and the surface at $b=\infty$ and $b=-\infty$ by double lines. In Figs. 1(d) and 1(i) some of the horizons are to be identified as shown. Some $b=$const surface are indicat-

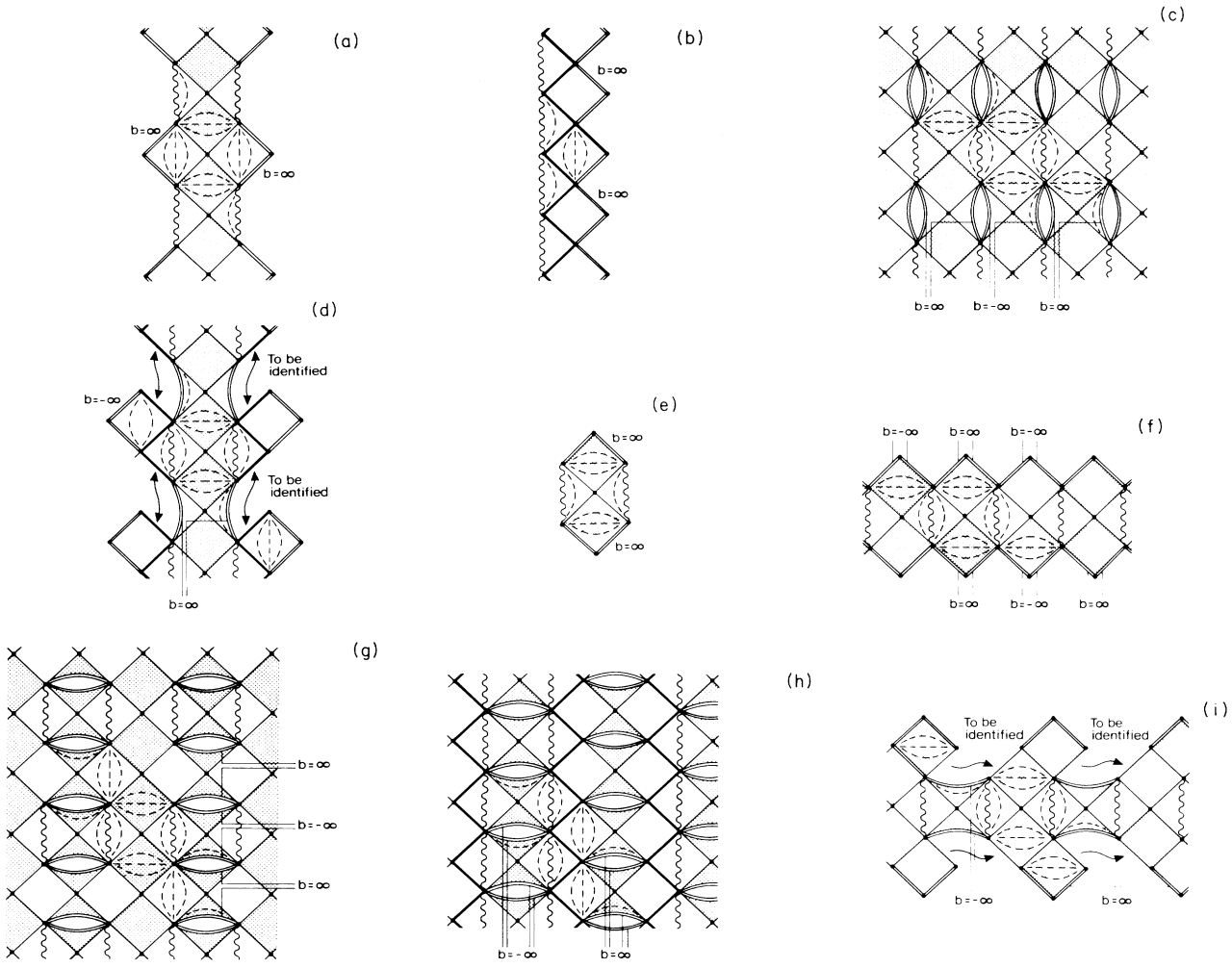

FIG. 1. Carter-Penrose diagrams for the $m=1$ solutions. (a) $k_b=1$, $G^2M^2>\kappa^2q_2{}^2$, and $\lambda_1<\Lambda\leq 0$; or $k_b=0$, $M\neq 0$, and $\lambda_1<\Lambda<0$; or $k_b=-1$, $M\neq 0$, and $\lambda_1<\Lambda<\lambda_2$. (b) $k_b=1$, $G^2M^2\geq\kappa^2q_2{}^2$, and $\Lambda=\lambda_1$; or $k_b=0$, $M\neq 0$, and $\Lambda=\lambda_1$; or $k_b=-1$ and $\Lambda=\lambda_1$. (c) $k_b=-1$ and $\lambda_2<\Lambda<0$. (d) $k_b=-1$ and $\Lambda=\lambda_2$. (e) $k_b=0$, $M\neq 0$, and $\Lambda=0$. (f) $k_b=1$, $G^2M^2\leq\kappa^2q_1{}^2$, and $\Lambda>0$; or $k_b=1$, $\kappa^2q_1{}^2<G^2M^2<\kappa^2q_2{}^2$, and $0<\Lambda<\lambda_1$; or $k_b=1$, $G^2M^2>\kappa^2q_1{}^2$, and $\Lambda>\lambda_2$; or $k_b=0$ and $\Lambda>0$; or $k_b=-1$ and $\Lambda\geq 0$. (g) $k_b=1$, $\kappa^2q_1{}^2<G^2M^2<\kappa^2q_2{}^2$, and $\lambda_1<\Lambda<\lambda_2$; or $G^2M^2\geq\kappa^2q_2{}^2$ and $0<\Lambda<\lambda_2$. (h) $k_b=1$, $\kappa^2q_1{}^2<G^2M^2<\kappa^2q_2{}^2$, and $\Lambda=\lambda_1$. (i) $k_b=1$, $G^2M^2>\kappa^2q_1{}^2$, and $\Lambda=\lambda_2$.

ed by the dotted lines. The shaded regions are those which correspond to cosmological solutions. In the degenerate cases shown in Figs. 1(b), 1(d), and 1(h) the cosmological region coincides with the horizon indicated by a bold line. In these cases b is static while a oscillates. The metric for the cosmological solutions in these cases may be obtained from (2.3) by a limiting procedure.[12] Carter-Penrose diagrams for the $q=0$, $\Lambda=0$ solutions have been given in Refs. 6–8.

The main point of this analysis is that in many of the cases the cosmological region described by (2.3) is an interior region of a d-dimensional black hole. In the $\Lambda=0$, $k_b=1$ case, for example, $b(t)$ oscillates between the horizons $b=b_1$, b_2, where

$$(b_{1,2})^{d-3}=GM\pm(G^2M^2-\kappa^2q_2{}^2)^{1/2} . \tag{2.7}$$

Since one would expect the Cauchy horizons to be unstable and turn into real curvature singularities if the metric were perturbed, as occurs in four dimensions,[13–15] life could not easily exist in such a universe. Indeed, the pathological nature of these universes can be seen directly if following Matzner and Mezzacappa[6,7] one introduces a d-dimensional dust field into the model. The dust has an energy-momentum tensor whose only nonvanishing component is

$$T_{00}=\rho(t) . \tag{2.8}$$

Energy-momentum conservation gives

$$\rho=\frac{(d-2)C}{2\kappa^2ab^{d-2}} , \tag{2.9}$$

where C is an arbitrary constant. The remaining equations may be readily integrated. We once again have $\dot{b}^2=\Delta$, and setting $a=z(t)\dot{b}$ and solving for $z(t)$ we find that

$$a=\Delta^{1/2}\left[z_0-C\int\frac{db}{b^{d-3}\Delta^{3/2}}\right] , \tag{2.10}$$

where z_0 is an arbitrary constant. Since $a(t)$ can shrink to zero at some time t_0 whereas $b(t)$ is always finite, $\rho(t)$ will diverge as $t\to t_0$ and thus give rise to a real curvature singularity. This singularity can occur before or after b reaches its maximum value, and it will occur without warning since b and $\dot{b}/b$ will be finite.

Matzner and Mezzacappa[7] make a comment noting that the results of Isihara[16] indicate that for a dust-filled universe with topology $\mathbb{R}\times S^3\times S^7$ ($q=0$), the singularity structure is the same as in the five-dimensional ($\mathbb{R}\times S^3\times S^1$) case. While this comment is true it nevertheless obscures an important difference between the two cases—namely, that in the case of Ishihara's solutions $\rho(t)$ diverges when the physical scale factor of the Universe also diverges (and the internal-space scale factor shrinks to zero). That is, the singularity is also a real curvature singularity for the vacuum solutions unlike the five-dimensional case. In fact, Ishihara's results would seem to indicate that in the case of arbitrary dimensions the solutions do not correspond to black-hole interiors.

III. THE $k_a=0$ PHASE SPACE

We will now turn to the study of cosmological models with the same fields as the model of Sec. II but in an arbitrary number of dimensions, i.e., we will consider the system (1.5) with $2\kappa^2V=\Lambda$, $f=1$, and $\sigma=0$. If, in addition, $k_a=0$, the problem is greatly simplified since equations (1.5) may then be reduced to a two-dimensional autonomous system whose properties can be studied by standard techniques. This is possible since (1.5g) may be regarded as a polynomial of degree n in $1/b^2$:

$$\frac{2\kappa^2q^2}{b^{2n}}-n(n-1)\frac{k_b}{b^2}+[2\Lambda-m(m-1)H^2-2mnHI-n(n-1)I^2]=0 . \tag{3.1}$$

One may solve for $1/b^2$ and substitute back into (1.5d) and (1.5e) to obtain a pair of differential equations involving H and I only. If $d=6$ and $n=2$, for example, the system is

$$\dot{H}=-\tfrac{9}{2}H^2-5HI-\tfrac{1}{2}I^2-\frac{1}{4\kappa^2q^2}+\Lambda \mp\frac{k_b}{4\kappa^2q^2}[k_b{}^2+4\kappa^2q^2(3H^2+6HI+I^2-\Lambda)]^{1/2} , \tag{3.2a}$$

$$\dot{I}=\tfrac{9}{2}H^2+6HI-\tfrac{1}{2}I^2+\frac{1}{4\kappa^2q^2}-\Lambda \pm\frac{k_b}{4\kappa^2q^2}[k_b{}^2+4\kappa^2q^2(3H^2+6HI+I^2-\Lambda)]^{1/2} . \tag{3.2b}$$

It is not possible to write down a general analytic solution to (3.1). Nevertheless, all the essential properties of the manifold defined by (3.1) can be derived. If n is even (odd) then (3.1) will have at most two (three) real solutions. For convenience we will assume that n is even for the remainder of this paper. For n even (3.1) has real solutions provided

$$1+\left[\frac{2\kappa^2q^2}{(n-1)^{2n-1}}\right]^{1/(n-1)}[m(m-1)H^2+2mnHI+n(n-1)I^2-2\Lambda]\geq 0 . \tag{3.3}$$

The surface defined by (3.1) is then a hyperboloid embedded in $\mathbb{R}^3$. Since for each value of H and I there will in general be two values of $1/b^2$ it is convenient to represent the phase surface by two copies of the plane $\mathbb{R}^2$ glued together along the boundary of a forbidden region. The forbidden region comprises those values of H and I for which the left-hand side of (3.3) is negative. This is seen in Fig. 2 which shows the phase portrait for the $m=1$, $\Lambda=0$ system studied in Sec. II.

Figure 2 illustrates many features which will be common to all the phase diagrams which will examine in this

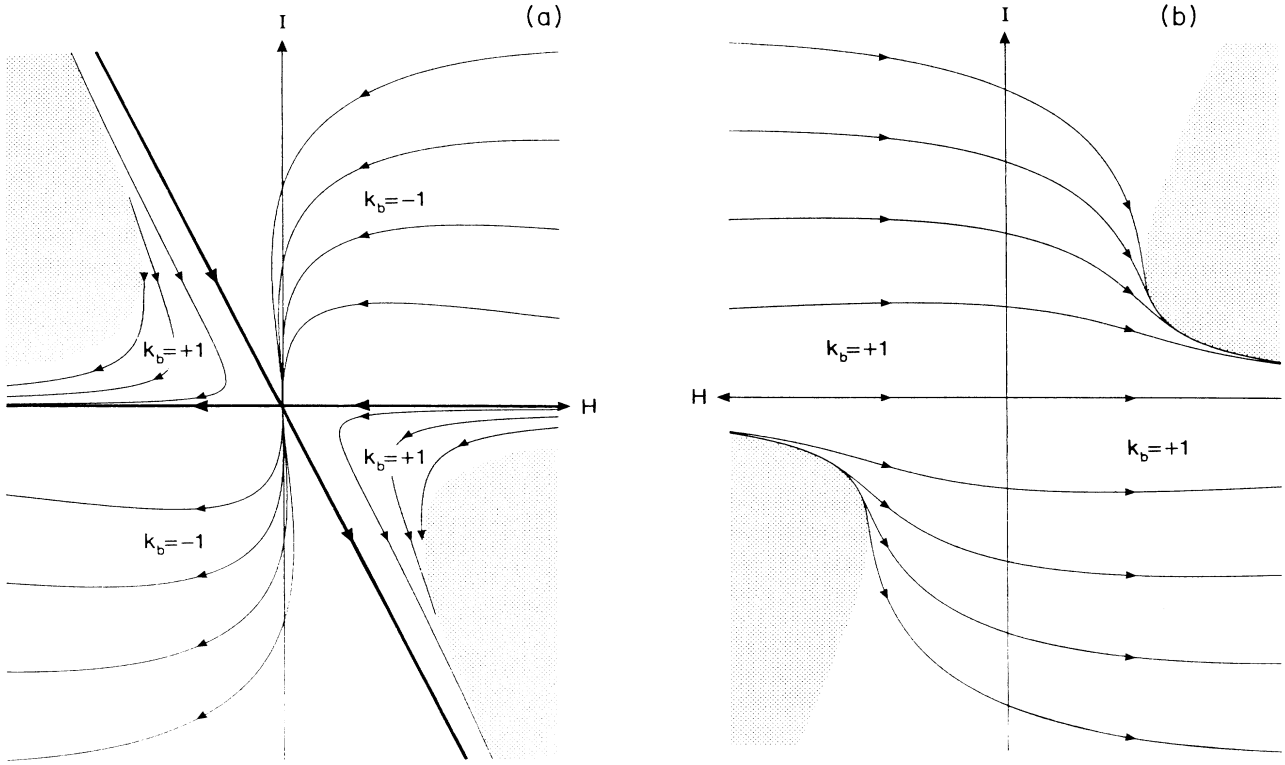

FIG. 2. The $m=1$, $\Lambda=0$ phase space: (a) lower branch; (b) upper branch.

section. It is divided into two regions: those corresponding to the $k_b=+1$ and $k_b=-1$ solutions. We have not shown the general $k_b=0$ solutions here; they fill the same region of the phase diagram as the $k_b=-1$ solutions. The separatrices which divide the $k_b=+1$ and $k_b=-1$ regions are the solutions for which $k_b=0$ and $q=0$. [They are indicated by the bold lines in Fig. 2(a).] In the $\Lambda=0$ case these separatrices are Kasner solutions.[17] In the $m=1$ case one of these solutions lies on the H axis, i.e., the internal space is static. The global nature of the spacetimes for the five-dimensional Kasner solutions was discussed in Ref. 8 and it is the same in the general $m=1$ case.

At a first glance one might be tempted to think that the boundary of the forbidden region is an allowed trajectory since the curve defined by (3.3) (in the case of equality) is a solution of the pair of equations for $\dot{H}$ and $\dot{I}$. However, there is a mathematical subtlety involved here. The Lipshitz condition, which guarantees the existence of a unique trajectory through each point of the phase space, is not satisfied on the boundary of the forbidden region. In (3.2), for example, this can be seen to be essentially because of the presence of the square-root factor. The boundary of the forbidden region is a solution in the same sense that the singular solution of Clairaut's equation is.[18] [For $m=1$ the singular "solution" corresponds to an infinite value of the integration constant M defined in (2.2).] In our case, however, we are really dealing with a three-dimensional phase space plus a constraint. At points on the boundary of the forbidden region solutions will have a nonzero velocity in the b dimension, which we have suppressed. The trajectories must therefore cross from one branch to the other and the singular solution is not allowed. Thus the $k_b=+1$ solutions in Fig. 2(a) which start close to the positive H axis [corresponding to the outer horizon in Fig. 1(a)] cross over to the other branch and head off in the direction of the negative H axis in Fig. 2(b) [which corresponds to the inner horizon in Fig. 1(a)]. [The positive H axis in Fig. 2(b) points in the opposite direction to that in Fig. 2(a).] We will henceforth call the branch containing the $k_b=0$ and $q=0$ separatrices the lower branch and the other branch (which contains $k_b=+1$ solutions only) the upper branch.

In Fig. 2 the only critical point is at the origin. (This is true also for arbitrary m if $\Lambda=0$.) This point is an attractor for $k_b=0,-1$ solutions with nonzero q [which occupy the upper right-hand side of Fig. 2(a)]. For the $k_b=0$ solutions (not shown here) a shrinks to zero at late times while $b\sim t^{2/(d-1)}$. In other words, these solutions become asymptotic to the Kasner solution with nonstatic b. The $k_b=-1$ solutions, on the other hand, approach the origin the origin along the I axis, i.e., $a\rightarrow$const and $b\sim t$ at late times. This is the Milne universe, which is just Minkowski space in unusual coordinates. The solutions which occupy the lower left-hand side of Fig. 2(a) are the time-reversed versions of the above solutions.

Figure 2 does have some features which do not generalize to the arbitrary m case. In particular, there is a

solution with b static on the upper branch as well as on the lower branch. This is the Robinson-Bertotti-type solution which corresponds to the neighborhood of the horizon in Fig. 1(b). Such a solution is present in all of the $m=1$ phase spaces if

$$\Lambda<\Lambda_1\equiv\left[\frac{(d-3)^{2d-5}}{2^{d-2}\kappa^2 q^2}\right]^{1/(d-3)} \tag{3.4}$$

[cf. Figs. 1(b), 1(d), and 1(h)].

The lower-branch phase diagrams for $m=1$ solutions with nonzero Λ are shown in Fig. 3. (The behavior of solutions on the upper branch is very similar to the $\Lambda=0$ case.) If $\Lambda<0$ there are no critical points—all solutions oscillate between the black-hole horizons (cf. Figs. 1(a)–1(d)]. If $\Lambda>0$ there are critical points $D_{1,2}$ at $H=I=[2\Lambda/(d-1)(d-2)]^{1/2}$. These are just the de Sitter solutions

$$\begin{aligned} a&=C_a\exp\left[\pm\left[\frac{2\Lambda}{(d-1)(d-2)}\right]^{1/2}t\right], \\ b&=C_b\exp\left[\pm\left[\frac{2\Lambda}{(d-1)(d-2)}\right]^{1/2}t\right], \end{aligned} \tag{3.5}$$

where C_a and C_b are arbitrary constants. The solution with the upper (lower) sign is an attractor (repellor) for all $k_b=-1$ and $k_b=0$ solutions with nonzero q. If $\Lambda>\Lambda_1$ this is also true for the $k_b=+1$ solutions with nonzero q [see Fig. 3(c)]. If $0<\Lambda<\Lambda_1$ the $k_b=+1$ solutions may either tend to the de Sitter attractor or else oscillate as in the $\Lambda<0$ case [see Fig. 3(b).] Trajectories displaying these two types of behavior are divided by a separatrix which passes through saddle points $C_{1,2}$ on the H axis [cf. Figs. 1(g)–1(i)]. In the critical case $\Lambda=\Lambda_1$ there is a single saddle point at the origin. In this case there is only one solution lying on the H axis (that is, with b static). It coincides with part of the boundary of the forbidden region and is the only trajectory in this case which does not tend to the de Sitter solution at late times. For this solution a grows as $a\sim t$, which corresponds to the Milne universe.

We will now examine the phase space of the solutions with n even and m arbitrary. The separatrices which divide the regions corresponding to $k_b=+1$ and $k_b=-1$ (or $k_b=0$, $q\neq 0$) are once again the $k_b=0$, $q=0$ solutions, which have been derived explicitly by Sato.[19] The solutions are

$$a=C_a t^{p_a},\quad b=C_b t^{p_b},\quad \Lambda=0\ , \tag{3.6}$$

$$a=C_a\,|\sin\tfrac{1}{2}\gamma t\,|^{p_a}\,|\cos\tfrac{1}{2}\gamma t\,|^{2/(d-1)-p_a},\quad \Lambda<0\ , \tag{3.7}$$

$$b=C_b\,|\sin\tfrac{1}{2}\gamma t\,|^{p_b}\,|\cos\tfrac{1}{2}\gamma t\,|^{2/(d-1)-p_b},\quad \Lambda<0\ ,$$

$$a=C_a\,|\sinh\tfrac{1}{2}\gamma t\,|^{p_a}\,|\cosh\tfrac{1}{2}\gamma t\,|^{2/(d-1)-p_a},\quad \Lambda>0\ , \tag{3.8}$$

$$b=C_b\,|\sinh\tfrac{1}{2}\gamma t\,|^{p_b}\,|\cosh\tfrac{1}{2}\gamma t\,|^{2/(d-1)-p_b},\quad \Lambda>0\ ,$$

where C_a and C_b are arbitrary constants.

$$\gamma^2=2\left[\frac{d-1}{d-2}\right]|\Lambda|\ , \tag{3.9}$$

and p_a and p_b satisfy the relations

$$mp_a+np_b=1,\quad mp_a{}^2+np_b{}^2=1\ . \tag{3.10}$$

The solutions (3.6) are the generalized Kasner solutions written down by Chodos and Detweiler.[17] The $\Lambda<0$ solutions (3.7) reduce to the Kasner solutions at times $|\gamma t|\ll 1$ or $|\pi-\gamma t|\ll 1$—they expand and recollapse in a finite time. The $\Lambda>0$ solutions reduce to the Kasner solutions at early times $|\gamma t|\ll 1$ and approach the de Sitter solution (3.5) at late times $|\gamma t|\gg 1$.

It is extremely useful to have an explicit solution for the $k_b=0$, $q=0$ separatrices since it turns out that the only critical points at the phase-space infinity lie on these separatrices. To see this it is convenient to use the standard technique of mapping the HI plane onto the lower half of a sphere of unit radius (the Poincaré sphere) which lies on the HI plane with the south pole touching the plane at the origin. The mapping is performed by means of a central projection. In our case a complete sphere is needed of course: one half-sphere for the lower branch and one half-sphere for the upper branch. The points at infinity are mapped onto the equator of the sphere by this procedure.

If one performs such an analysis one finds that in our case there are four critical points at infinity: two nodes N_1,N_2 at

$$H=\pm\infty,\quad I=\frac{p_{b+}}{p_{a+}}H\ , \tag{3.11}$$

and two saddle points S_1,S_2 at

$$H=\pm\infty,\quad I=\frac{p_{b-}}{p_{a-}}H\ , \tag{3.12}$$

where $p_{a\pm}$ and $p_{b\pm}$ are the solutions of (3.10):

$$\begin{aligned} p_{a\pm}&=\frac{1}{m+n}\left[1\pm\left[\frac{n(d-2)}{m}\right]^{1/2}\right], \\ p_{b\pm}&=\frac{1}{m+n}\left[1\mp\left[\frac{m(d-2)}{n}\right]^{1/2}\right]. \end{aligned} \tag{3.13}$$

These points lie on the $k_b=0$, $q=0$ separatrices at infinity and are shown in Fig. 4 which is the vertical projection onto the HI plane from the half-sphere corresponding to the lower branch. Since these points are Kasner-type singularities for all values of Λ, if $m\neq 1$ and $n\neq 1$ then the resulting behavior of a and b will lead to real curvature singularities of the metric. At the nodes, for example, $a\to 0$, $\dot{a}\to\infty$, $b\to\infty$, and $\dot{b}\to-\infty$. For the $k_a=0$ solutions at least, therefore, the spacetimes (1.1) do not in general correspond to black-hole interiors.

To determine the overall structure of the phase space one must also locate the critical points at finite values of H and I. The number and nature of the critical points varies as Λ varies. The bifurcation values are

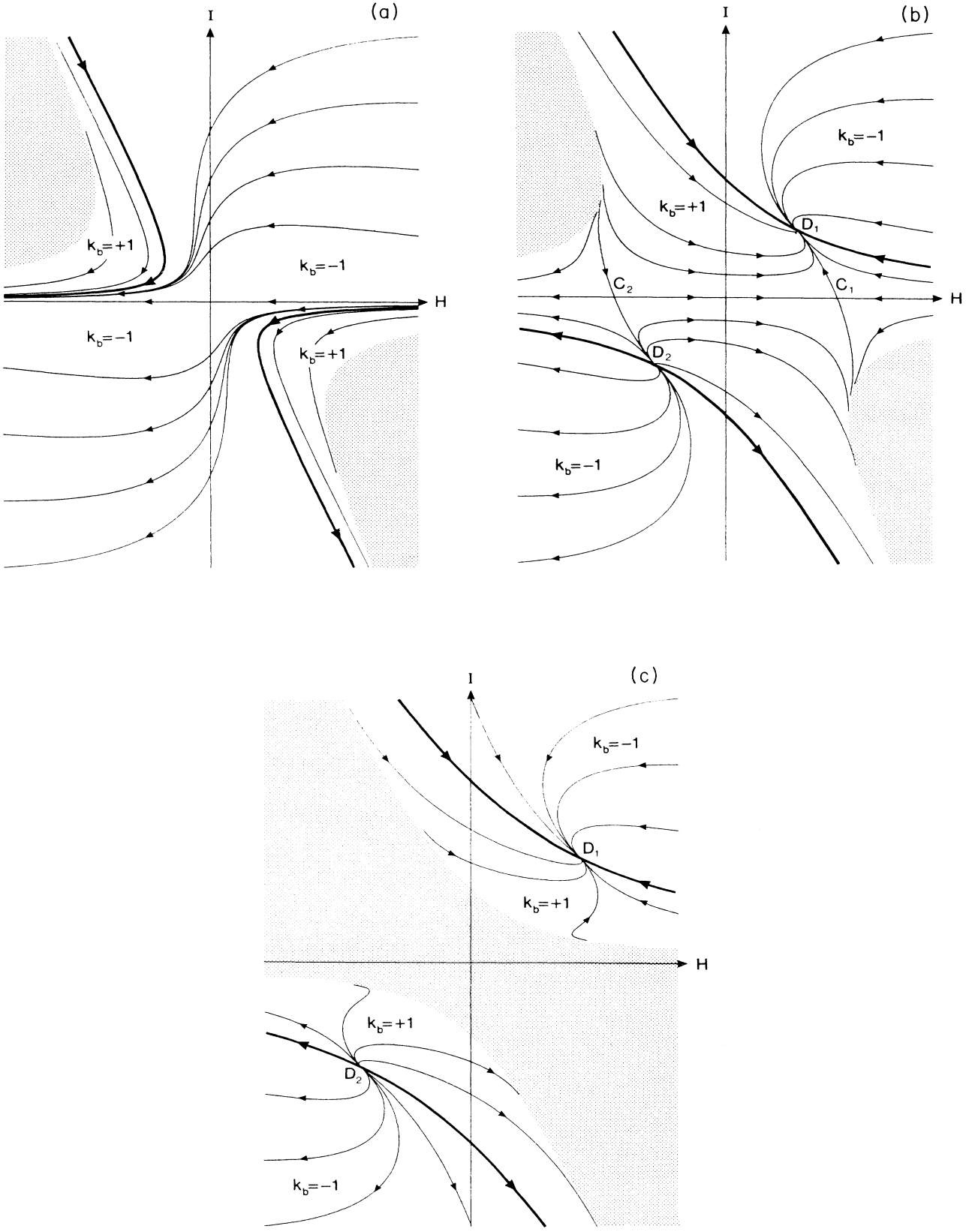

FIG. 3. The lower branch of the $m=1$ phase space: (a) $\Lambda<0$; (b) $0<\Lambda<\Lambda_1$; (c) $\Lambda>\Lambda_1$.

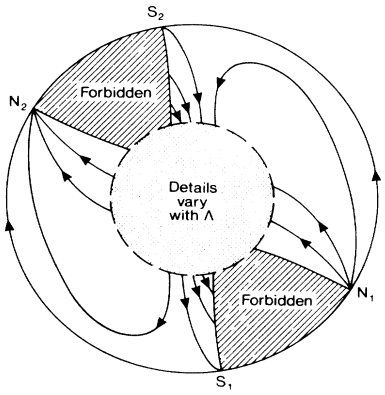

FIG. 4. The vertical projection of the Poincaré sphere for the lower branch onto the H,I plane for the general $k_a=0$ system. The nodes N_1 and N_2 and saddle points S_1 and S_2 are Kasner singularities.

$$\Lambda_0=0\ ,$$
$$\Lambda_1=\left[\frac{(n-1)^{2n-1}}{2^n\kappa^2q^2}\right]^{1/(n-1)}\ , \tag{3.14}$$
$$\Lambda_2=\left[\frac{(d-2)^n(n-1)^{2n-1}}{(2n)^nm\kappa^2q^2}\right]^{1/(n-1)}\ .$$

We will examine the distinct cases in turn.

$\Lambda=0$. The phase diagram for this case is shown in Fig. 5. All solutions with nonzero q (and $H>0$ initially) begin at the Kasner singularity N_1. (This is true for all values of Λ.) As in the $m=1$ case the only critical point is at the origin and it is an attractor for all $k_b=-1$ and $k_b=0$ solutions with nonzero q (and $H>0$ initially). Thus the $k_b=-1$ solutions approach the Milne universe at late times. For the $k_b=0$ solutions $a\sim t^{p_a-}$ and $b\sim t^{p_b-}$ at late times. Thus for these solutions a shrinks while b blows up. The $k_b=+1$ trajectories leave the initial singularity on the lower branch, cross to the upper branch, cross back to the lower branch and reach the Kasner singularity N_2 in a finite time. This corresponds to a expanding from zero to a maximum and recollapsing in a big crunch. At the same time b contracts from an infinite value to a minimum value and finally blows up again.

This property of one of the scale factors collapsing in a finite time while the other scale factor grows infinite simultaneously appears to remain a feature of models which contain higher-dimensional matter in the form of a perfect fluid, dust or a scalar field.[16,20–25] Such models lack a solution with a flat Minkowski physical space and static internal space. In Refs. 20–25 the authors took the view that the collapsing scale factor corresponds to the internal space and the expanding scale factor to the physical space (a reversal of their roles with respect to our models[26]). To obtain a realistic universe the internal space should then be stabilized by quantum effects before the singularity is reached while the physical universe should go over to the standard Friedman-Robertson-

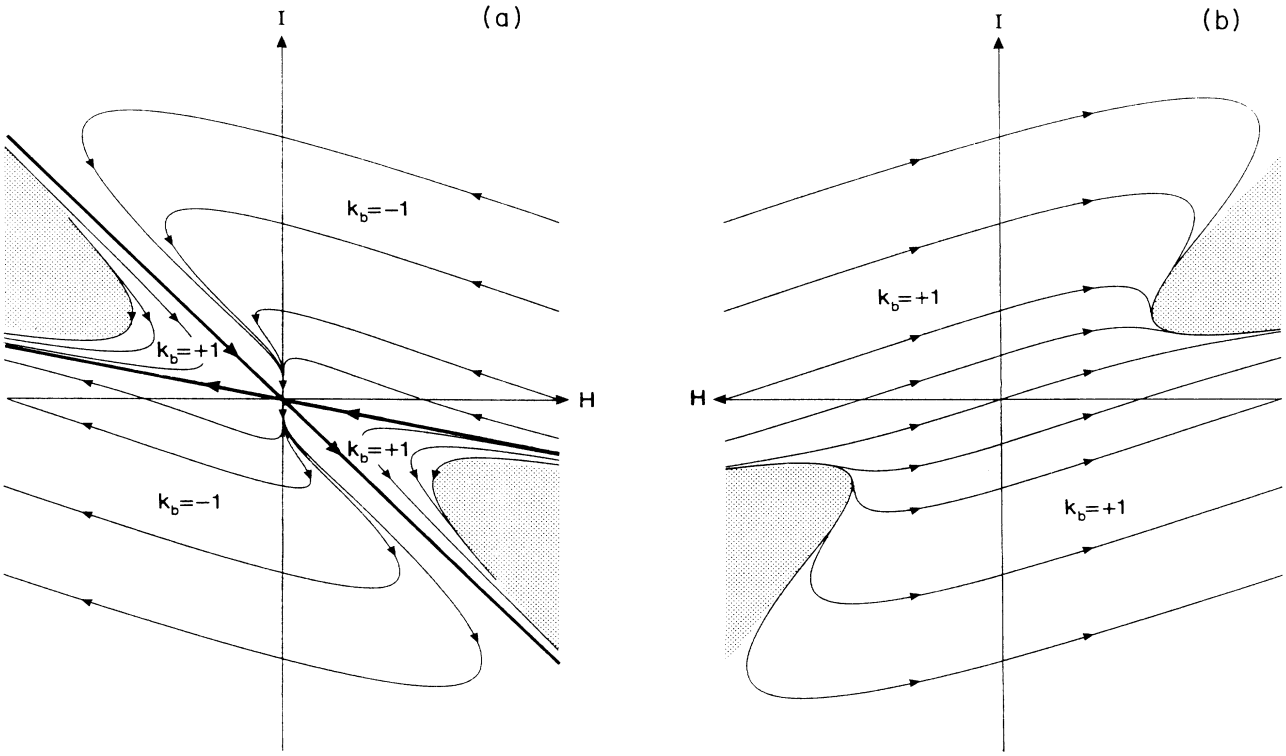

FIG. 5. The phase space for the general $k_a=0$ system with $\Lambda=0$: (a) lower branch; (b) upper branch.

Walker behavior. However, as can be seen from Fig. 5, such a scenario is not admitted by the Freund-Rubin mechanism unless Λ is fine-tuned to some particular value.

$\Lambda<0$. The lower branch of the phase diagram is shown in Fig. 6(a) [the upper branch being similar to Fig. 5(b)]. All solutions with nonzero q undergo the same behavior as the $k_b=+1$ solutions in the $\Lambda=0$ case: the physical space expands from the initial Kasner singularity and recollapses to the final Kasner singularity in a finite time.

$\Lambda>0$. For all values of $\Lambda>0$ there are critical points $D_{1,2}$ at the de Sitter values

$$H=I=\left[\frac{2\Lambda}{(d-1)(d-2)}\right]^{1/2}.$$

The de Sitter solution (3.6) is an attractor for all $k_b=-1$ and $k_b=0$ solutions with nonzero q. If $\Lambda>\Lambda_2$ it is also an attractor for all $k_b=+1$ solutions with nonzero q [see Fig. 6(e)]. If $0<\Lambda<\Lambda_2$ there can be as many as four additional critical points—these all lie on the H axis and are given by solutions of the equation

$$2\kappa^2q^2(2\Lambda-m^2H_0^2)^n+(n-1)^{2n-1}[m(d-2)H_0^2-2\Lambda]=0. \quad (3.15)$$

If $0<\Lambda<\Lambda_1$, then (3.15) has two saddle-point solutions $C_{1,2}$: one on the positive H axis and one on the negative H axis [see Fig. 6(b)]. Separatrices which pass through these saddle points divide trajectories which approach the de Sitter solution at late times from those that reach the final Kasner singularity N_2 in a finite time.

If $\Lambda_1<\Lambda<\Lambda_2$ then (3.15) has four solutions: in addition to the two saddle points of the previous case there is an asymptotically stable attractor A_1 on the positive H axis and a repellor A_2 on the negative H axis [see Fig. 6(d)]. For $\Lambda>\Lambda_1$ the phase hyperboloid splits into two sheets. Thus, trajectories which leave the initial Kasner singularity N_1 cannot reach the final singularity N_2. For $\Lambda_1<\Lambda<\Lambda_2$, the separatrices which pass through the saddle points divide trajectories which approach the de Sitter solution at late times from those that approach the attractor on the H axis at late times. (The trajectories on the other sheet of the hyperboloid are just the time reversed solutions.) If $\Lambda_1<\Lambda<\Lambda_{3/2}$, where

$$\Lambda_{3/2}=9\left[\frac{(d-2)^n(n-1)^{2n-1}(m+8)}{2^nm[(d-2)+8n]^n\kappa^2q^2}\right]^{1/(n-1)} \quad (3.16)$$

then the attractor is a spiral point. If $\Lambda_{3/2}\le\Lambda<\Lambda_2$ then it is a node. Although this attractor has a static internal space the solutions which reach it are not physically relevant since a grows exponentially at late times. In the critical case $\Lambda=\Lambda_2$ the saddle points and attractor (repellor) coalesce to give one critical point on the positive H axis and one on the negative H axis. One may verify numerically that the resulting critical point on the posi-

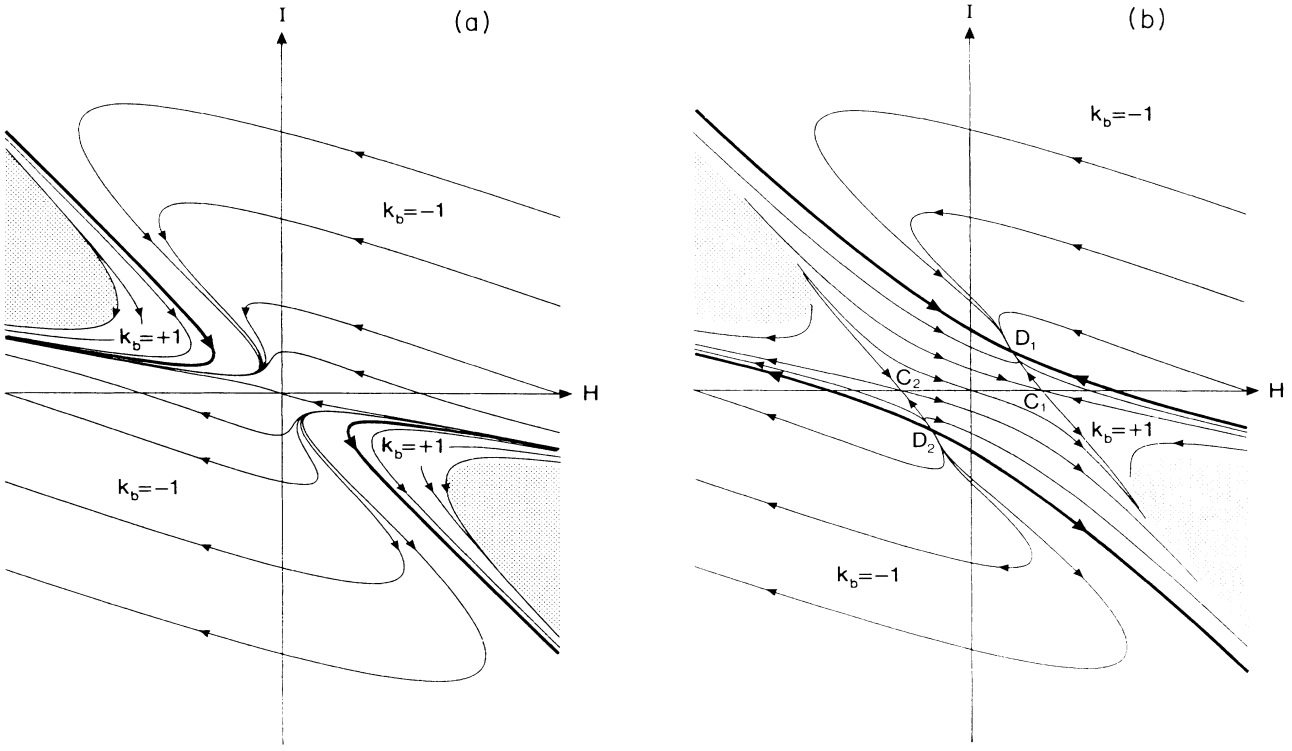

FIG. 6. The lower branch of the general $k_a=0$ phase space: (a) $\Lambda<0$; (b) $0<\Lambda<\Lambda_1$; (c) $\Lambda=\Lambda_1$; (d) $\Lambda_1<\Lambda\le\Lambda_2$; (e) $\Lambda>\Lambda_2$.

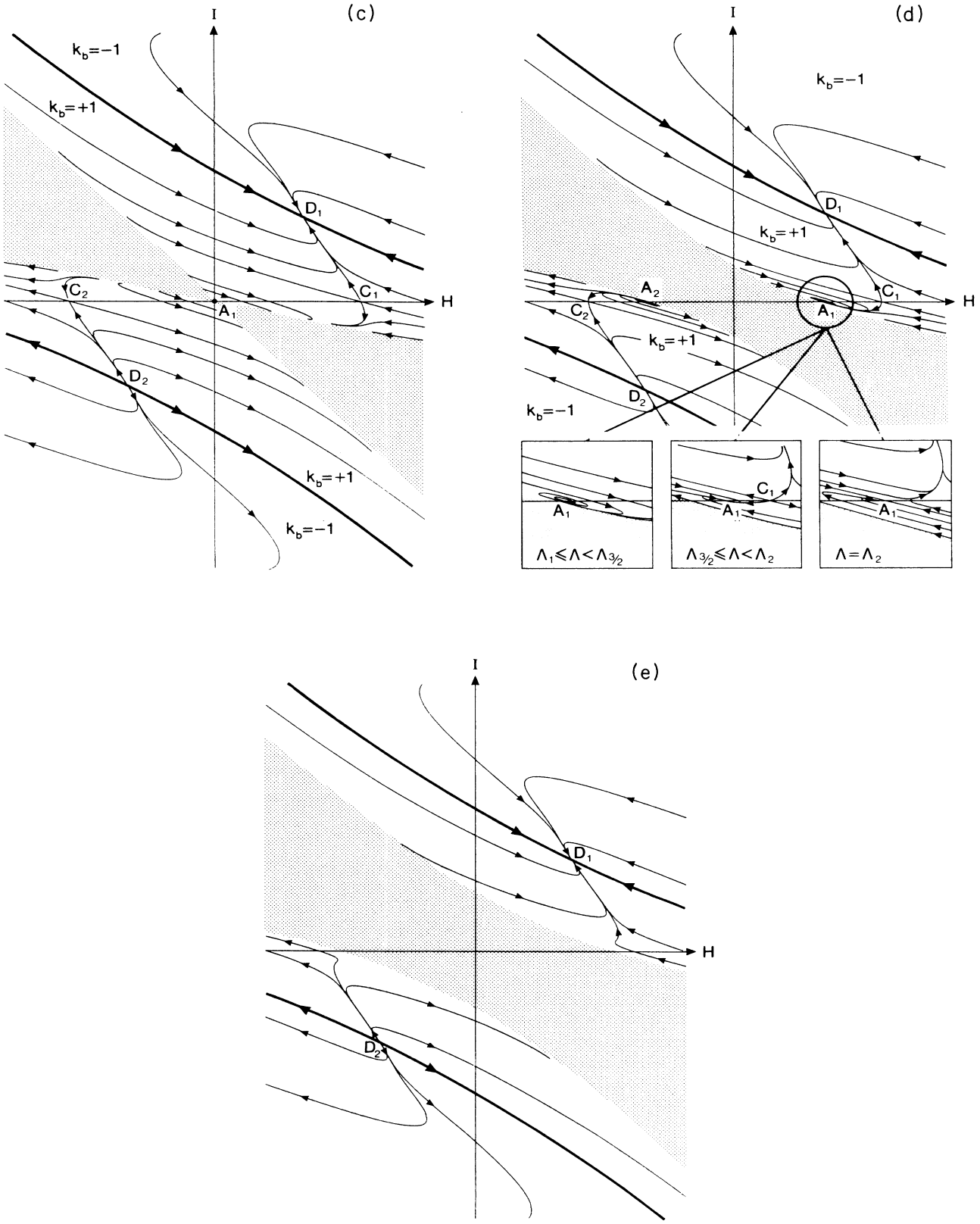

FIG. 6. (*Continued*).

tive H axis is still an asymptotically stable attractor.

In the other critical case $\Lambda=\Lambda_1$, there is a single critical point at the origin in addition to the two saddle points [see Fig. 6(c)]. This is an asymptotically stable spiral point for some $k_b=+1$ solutions starting out from the initial singularity N_1. (It is a repellor for the time-reversed solutions.) Since both a and b are static at late times this corresponds to a universe with a $M^4\times B^n$ vacuum (where B^n is any Einstein space of positive curvature). It is therefore of more physical interest than the other cases even though one must fine-tune Λ to obtain the desired behavior. This case has been studied previously by Okada.[27,28]

At a first glance there appears to be an additional pair of critical points if $\Lambda>0$. However, these lie on the boundary of the forbidden region, and just as the boundary is not a true trajectory these points are not true critical points.

IV. THE PHASE SPACE FOR OPEN AND CLOSED MODELS

To discuss the solutions with $k_a\neq 0$ it is convenient to work with a new variable J defined by $J\equiv 2\kappa^2 q^2/b^{2n}$ rather than with b. The critical points corresponding to the late-time behavior of the solutions are then located at finite values in the H,I,J phase space. The constraint (1.5g) may be used to eliminate a^2 from the other differential equations (1.5). The system is therefore described by the equations

$$\dot{H}=-H^2+nHI+\frac{n}{m}(n-1)I^2+\frac{n(n-1)k_b}{2m\kappa^2q^2}J^{2/n}-\frac{mn+n-1}{m(d-2)}J^2-\frac{2(n-1)\Lambda}{m(d-2)}\ , \tag{4.1a}$$

$$\dot{I}=-mHI-nI^2-\frac{(n-1)k_b}{2\kappa^2q^2}J^{2/n}+\frac{m}{d-2}J^2+\frac{2\Lambda}{d-2}\ , \tag{4.1b}$$

$$\dot{J}=-nIJ\ . \tag{4.1c}$$

Trajectories cannot cross the $J=0$ plane. The $J=0$ system corresponds physically to a universe with $k_b=0$ and $q=0$. Since we are only interested in solutions with $b>0$ ($J\geq 0$) (the solutions with $b<0$ being qualitatively the same), it is convenient to represent the $J\geq 0$ regions of the $k_b=+1$ and $k_b=-1$ solutions in a single diagram by using a coordinate $J'\equiv k_bJ$. The $k_a=0$ phase diagrams drawn in the last section correspond to the surface of a hyperboloid embedded in this combined phase space. The $k_a=-1$ and $k_a=+1$ solutions correspond to the interior and exterior of the hyperboloid, respectively. (We could replace the $k_b=-1$ half of the diagram by the $J\geq 0$ portion of the $k_b=0$ phase space if we so wished. The qualitative features such as the number and nature of the critical points would be the same, although the $k_b=0$ solutions would approach the critical points from a different direction.)

The $J=0$ phase planes are sketched in Fig. 7. Since $q=0$ for these solutions there is no compactification mechanism and the scale factors a and b have a more equal footing. This can be seen from the fact that the critical points at infinity S_1 and S_2 which were saddle points with respect to solutions lying on the $k_a=0$ hyperboloid are nodes with respect to solutions lying in the $J=0$ surface. Thus in the $\Lambda<0$ case, for example there are two-dimensional sets of solutions for which a shrinks to zero and b blows up in a finite time and also for which b shrinks to zero while a blows up. For $\Lambda=0$ the $k_a=-1$ solutions approach the Milne universe at late times. (This case was discussed in Ref. 8.) If $\Lambda>0$ the $k_a=-1$ trajectories approach the de Sitter solution at late times. Some $k_a=+1$ trajectories also approach the de Sitter solution. They are divided from the trajectories which travel from N_1 to N_2 in a finite time by separatrices which pass through the saddle points $B_{1,2}$. These separatrices also divide off trajectories which travel from N_1 to S_1 and from S_2 to N_2; i.e., one scale factor starts from zero and goes infinite in a finite time while the other scale factor starts infinite and simultaneously shrinks to zero. The saddle points B_1 and B_2 are the only critical points at finite values of H,I,J besides those lying on the $k_a=0$ hyperboloid. They are located at

$$H=J=0,\quad I=\pm\left[\frac{2\Lambda}{n(d-2)}\right]^{1/2},\quad \Lambda\geq 0\ . \tag{4.2}$$

In the case of the critical points lying on the $k_a=0$ hyperboloid the dimension of the set of solutions entering (leaving) points with $H>0$ ($H<0$) is increased by one in the three-dimensional phase space. Thus both A_1 and D_1 are still attractors in the three-dimensional phase space, while C_1 attracts a two-dimensional bunch of trajectories. The saddle point B_1 similarly attracts a two-dimensional bunch of trajectories.

To examine the critical points at infinity in the full three-dimensional phase space it is convenient to use the procedure of Belinsky *et al.*[9] One first transforms to spherical polar coordinates r,θ,ϕ defined by

$$H=r\sin\theta\cos\phi,\quad I=r\sin\theta\sin\phi,\quad J=r\cos\theta\ , \tag{4.3}$$

and then brings the sphere at infinity to a finite distance from the origin by the transformation $r=\rho(1-\rho)^{-1}$, $0\leq\rho\leq 1$. The critical points at infinity ($\rho=1$) are then determined from the resulting equations for $d\rho/d\tau$, $d\theta/d\tau$, and $d\phi/d\tau$, where τ is a new time coordinate defined by $d\tau=rdt$. One finds that apart from the critical points $N_{1,2}$ and $S_{1,2}$ which lie on the $k_a=0$ hyperboloid the only critical points at infinity are saddle points in the $k_a=-1$ models. These are the points $S_{3,4}$ located at

$$\theta=\pi/2,\quad \phi=0,\pi\ \text{ or }\ H=\pm\infty,\quad I=J=0\ , \tag{4.4}$$

and the points $S_{5\pm,6\pm}$ located at

$$\theta=\arctan\pm\left[\frac{n^2+1}{n(d-2)}\right]^{1/2},\quad \phi=\arctan\frac{1}{n}$$

or

$$H=\pm\infty,\quad I=\frac{1}{n}H,\quad J=\pm\left[\frac{d-2}{n}\right]^{1/2}H\ . \tag{4.5}$$

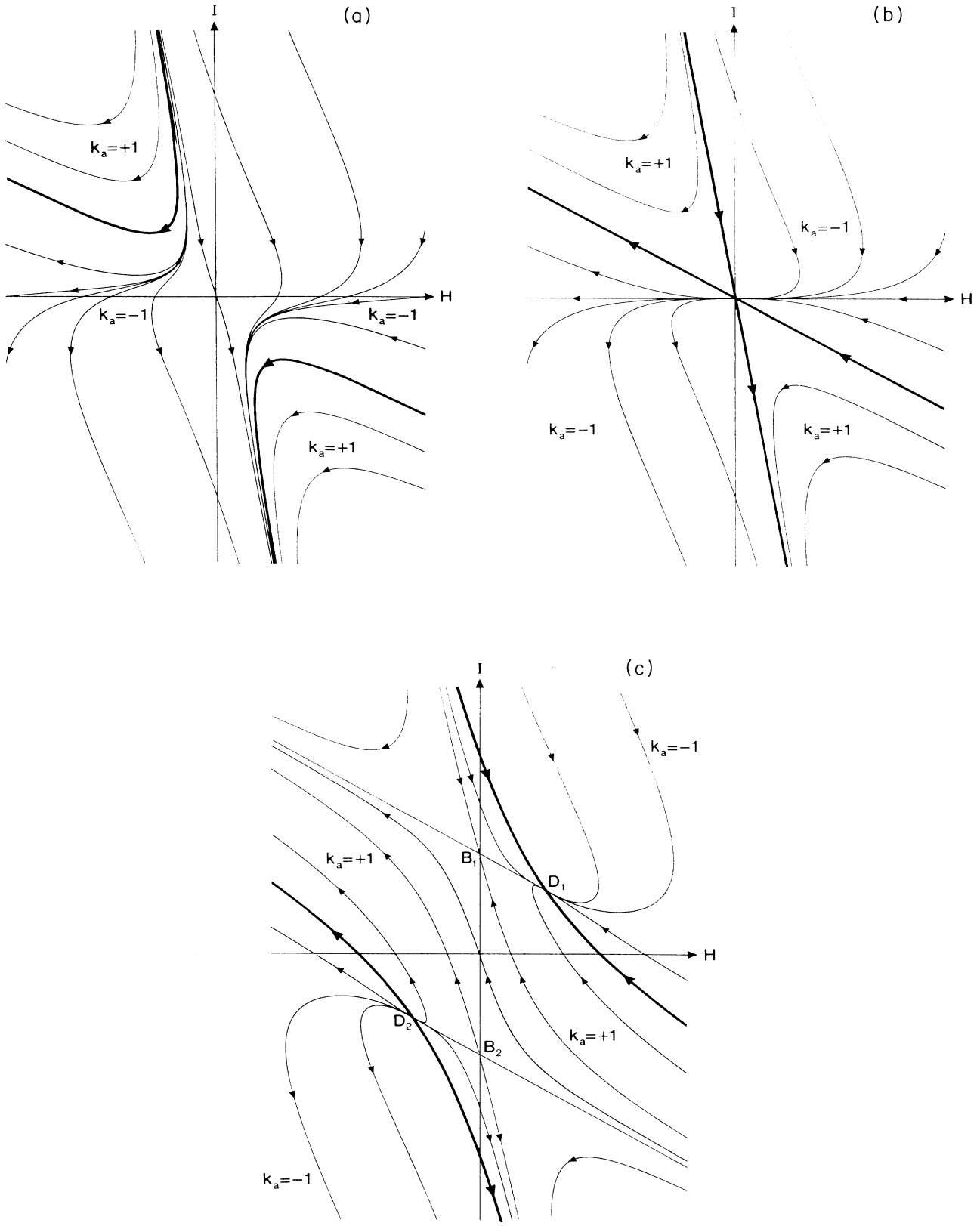

FIG. 7. The $J=0$ phase space: (a) $\Lambda<0$; (b) $\Lambda=0$; (c) $\Lambda>0$.

(We assume that S_3 and $S_{5\pm}$ are given by the points with $H>0$ and S_4 and $S_{6\pm}$ by the points with $H<0$.) These points are present in all $k_a=-1$ models regardless of the value of k_b.

An analysis of small perturbations about the critical points reveals that $N_{1,2}$ are still nodes in the full three-dimensional phase space. Thus N_1 ejects trajectories into all models $k_a,k_b=+1,0,-1$. The saddle point S_1 attracts a two-dimensional bunch of trajectories and S_2 repells a two-dimensional bunch of trajectories: those lying on the $J=0$ plane (see Fig. 7). The saddle point S_3 (S_4) similarly repels (attracts) a two-dimensional bunch of solutions which travel to finite values of H, I, and J. A single trajectory leaves (enters) the points $S_{5\pm}(S_{6\pm})$ traveling to (from) finite values of H, I, and J.

The asymptotic behavior (for $|t|\ll 1$) of solutions near the critical points S_{3-6} of the $k_a=-1$ models is as follows: near $S_{3,4}$ $a\sim t$ and $b\rightarrow$const; and near $S_{5\pm,6\pm}$, $a\sim t$ and $b\sim t^{1/n}$. The points S_3 and S_4 are not curvature singularities and will correspond to horizons. There can therefore be cases in which spacetimes similar to those of the $m=1$ solutions are encountered. However, this is only true for at most a two-dimensional bunch of trajectories. The behavior is not stable in the three-dimensional space of all trajectories. Thus our remarks made in Sec. III are quite general: Kaluza-Klein cosmological solutions do not, in general, correspond to black-hole interiors.

In addition to the trajectories which travel from the sphere at infinity to finite values of H, I, and J there are trajectories which lie entirely on the $\rho=1$ surface. Although these trajectories are unphysical it is helpful to sketch them since by continuity arguments they will determine the behavior of the physical integral curves which lie within the sphere at infinity but near its surface. Such a diagram is reproduced in Fig. 8, where we have sketched the $\rho=1$ surface treating the polar angles θ and ϕ as Cartesian coordinates. The curved trajectories which join S_1 with N_2 and N_1 with S_2 represent the projection of the $k_a=0$ hyperboloid onto the sphere at infinity.

To complete this section we will summarize the overall behavior of all the trajectories. Apart from the various one- and two-dimensional bunches of solutions in the $k_a=-1$ models and the $J=0$ plane, all solutions (with $H>0$ initially) start from the singularity N_1. The behavior of these (nonzero q) solutions at late times depends on Λ and is as follows.

$\Lambda<0$. All trajectories (with nonzero q) travel to the singularity N_2 in a finite time.

$\Lambda=0$. All trajectories with $k_a=+1$ or $k_b=+1$ travel to the singularity N_2 in a finite time. If $k_a=0$ or -1 and $k_b=0$ or -1 all trajectories approach the origin $H=I=J=0$ at late times.

$\Lambda>0$. If $k_a=0$ or -1 and $k_b=0$ or -1 all trajectories approach the de Sitter solution at late times. If $k_a=+1$ then for all positive values of Λ there will be solutions which travel to the singularity N_2 in a finite time (whether $k_b=+1,0$ or -1). Let us denote this three-dimensional set of solutions G_1. They will be separated from trajectories with other behavior by two two-dimensional separatrices of trajectories which travel from N_1 to B_1 and from B_2 to N_2. Let us denote the second three-dimensional set of trajectories by G_2. The set G_2 will be divided into two further sets of trajectories if $0<\Lambda\leq\Lambda_2$.

If $0<\Lambda<\Lambda_1$ a two-dimensional separatrix of trajectories traveling from N_1 to C_1 divides G_2 into a three-dimensional set of trajectories which travel to N_2 in a finite time (like the G_1 solutions) and a three-dimensional set of trajectories which approach the de Sitter solution at late times. If $\Lambda_1<\Lambda\leq\Lambda_2$ the two-dimensional separatrix of trajectories traveling from N_1 to C_1 will divide a three-dimensional set of trajectories which approach the attractor A_1 at late times from a set which approach the de Sitter solution. If $\Lambda>\Lambda_2$ then all trajectories belonging to the set G_2 will approach the de Sitter solution at late times. If $k_a=0$ or -1 and

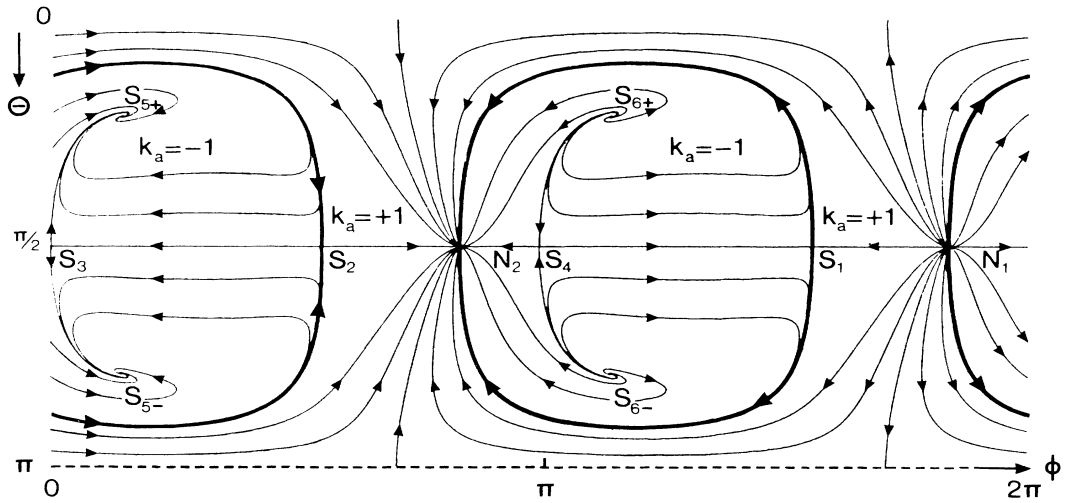

FIG. 8. The pattern of trajectories on the surface of the sphere at infinity for the general system.

$k_b=+1$ there will also exist a set of trajectories G_2 with the same properties as the set G_2 in the $k_a=+1$ case.

The solutions belonging to the set G_2 have been studied numerically by Forgács and Horváth[29] and Okada[27] for the $k_a=k_b=+1$ system in the fine-tuning case in six dimensions. Okada has also studied more general fine-tuning solutions (with $k_a=+1,0$ or -1) which include thermal and quantum effects as well as the Freund-Rubin mechanism.[28] His results show that the trajectories still have much the same qualitative behavior.

V. MODELS WITH DILATONS

Let us consider the case in which a scalar field is added to the model of the last section without any coupling to the Freund-Rubin field, i.e., $2\kappa^2 V=\Lambda$ and $f=1$. This is the next simplest case to consider since Eqs. (1.5) can then be reduced to a four-dimensional system. This can be achieved by using the constraint (1.5g) to eliminate a^2 from the right-hand side of the other equations, as in Sec. IV. Since trajectories cannot cross the $K=0$ subspace it seems likely that the behavior of solutions at late times will be very much the same to that encountered in the last section. The exact properties of all trajectories are difficult to determine because of the large dimensionality of the phase space. Some comments can be made nevertheless.

In addition to the critical points lying in the $K=0$ subspace, the only critical points at a finite distance from the origin of the four-dimensional phase space are saddle points in the $k_a=+1$ models, which are present if $\Lambda_1\le\Lambda\le\Lambda_2$. There are four such points: two at positive values of K and two at negative K. They are given by the solutions of the equations

$$H=I=0\ ,$$
$$\frac{m}{d-2}J^2-\frac{(n-1)k_b}{2\kappa^2 q^2}J^{2/n}+\frac{2\Lambda}{d-2}=0\ , \tag{5.1}$$
$$K^2=\frac{2\Lambda}{d-2}-\left[\frac{n-1}{d-2}\right]J^2\ .$$

Both critical points attract a two-dimensional bunch of trajectories. Evidently these bunches form separatrices though their role is not immediately clear. The dimension of the set of trajectories attracted to critical points with $H>0$ or $I>0$ which lie in the $K=0$ subspace is greater by one in the full four-dimensional phase space. (The dimension of the set of trajectories repelled by critical points with $H<0$ or $I<0$ is likewise greater by one.) Thus the points A_1 and D_1 are still asymptotically stable attractors.

It is once again possible to explicitly derive the $k_a=0$, $k_b=0$, $q=0$ solutions. One finds that

$$\sqrt{2}\kappa\sigma=\begin{cases}p_\sigma\ln|\tan\frac{1}{2}\gamma t|\ , & \Lambda<0\ ,\\ p_\sigma\ln|t|\ , & \Lambda=0\ ,\\ p_\sigma\ln|\tanh\frac{1}{2}\gamma t|\ , & \Lambda>0\ ,\end{cases} \tag{5.2}$$

while a and b are still given by the relations (3.6)–(3.8). The constants p_a, p_b, and p_σ now satisfy the conditions

$$mp_a+np_b=1,\quad mp_a^2+np_b^2+p_\sigma^2=1\ . \tag{5.3}$$

These solutions will form separatrices in the full four-dimensional phase space. The scale factors a, b and $e^{\sqrt{2}\kappa\sigma}$ all have a power-law behavior when $|\gamma t|\ll 1$ (and $|\pi-\gamma t|$ if $\Lambda<0$). If $\Lambda>0$ then a and b will approach the de Sitter solution (3.5) at late times.

An analysis of the critical points at infinity reveals that the nodes $N_{1,2}$ and saddles $S_{1,2}$ are members of a one-parameter set of critical points at infinity. These points are just those which correspond to the $k_a=0$, $k_b=0$, $q=0$ solutions (3.6)–(3.8), (5.2), and (5.3) with $|\gamma t|\ll 1$. They will always correspond to curvature singularities if $p_\sigma\neq 0$. These points are the only critical points at infinity apart from those for the $k_a=-1$ models which lie in the $K=0$ subspace. The global properties of the solutions with dilatons must therefore have much of the same global properties as the solutions without dilatons for this model.

A physically more interesting model containing a dilaton is that of $N=2$ gauged supergravity in six dimensions.[30,31] In this model there is a nontrivial coupling between the dilaton and Maxwell field, $f\equiv e^{\sqrt{2}\kappa\sigma}$, and an exponential potential $V\equiv(g_e^2/2\kappa^2)e^{-\sqrt{2}\kappa\sigma}$, where g_e is a coupling constant. The charge q is related to g_e by

$$q=\pm\frac{p}{2g_e}\ , \tag{5.4}$$

where p is restricted to be an integer by the requirement that gauge transformations be single valued. There has been considerable interest in the cosmological solutions of this model.[8,32–35]

The model admits a $M^4\times B^2$ solution if $p=1$. The phase space then has critical points at

$$H=I=K=0,\quad 1/b^2=2\kappa^{-2}g_e^2e^{-\sqrt{2}\kappa\sigma_0}\ , \tag{5.5}$$

with σ_0 arbitrary. (The fact that the critical points may have arbitrary σ is due to the scale invariance of the model.[8]) This "string" singularity appears to be an attractor for $k_a=0$ and $k_a=-1$ solutions with compact internal spaces.[33,35] There are no other critical points for finite values of the parameters.

The phase space for the system is five-dimensional since σ appears explicitly in the equations. Thus the overall behavior of the trajectories will be far more complex than in the models we have already encountered. Moreover, trajectories can now cross the $K=0$ subspace so the phase space will have rather different properties than those of the previous models. One may understand this difference physically as being a result of the scale invariance of the supersymmetric model. Halliwell has analyzed the phase space of $k_a=+1$ solutions in certain regions where various approximations hold.[35,36] Any more detailed analysis of the phase space would appear to be quite difficult.

VI. CONCLUSION

An analysis of the phase space of Kaluza-Klein cosmologies with Freund-Rubin compactification and an arbitrary cosmological constant reveals that the bizarre

behavior of the five-dimensional cosmologies[6–8] does not generalize to many other cases. Solutions in which either the physical or internal space has a single spatial dimension will correspond to black-hole interiors and will display pathological behavior. However, this behavior is not at all general: the only other case where it is possible is for a two-dimensional bunch of trajectories in the $k_a = -1$ models. If a dilaton is added to the model the properties of the solutions are much the same. In the case of the scale-invariant models, however, the phase space exhibits quite different behavior.

The most physically relevant case among the solutions we have discussed in detail is the fine-tuning case $\Lambda = \Lambda_1$. Trajectories in this model which pass very close to the saddle point C_1 will experience a long period of exponential inflation. The Hartle-Hawking proposal for the wave function of the Universe[37] may be applied to obtain initial conditions for the classical trajectories. Halliwell has calculated a minisuperspace wave function for the fine-tuning model in six dimensions.[38] The classical trajectories picked out by the Hartle-Hawking proposal in this case are those which start near C_1 and undergo a period of inflation. This set includes trajectories which approach the de Sitter solution D_1 at late times as well as those that approach the attractor A_1. To obtain enough inflation to solve the flatness problem it is necessary to tune the initial conditions to an extremely high accuracy, however, and the model cannot be regarded as a true inflationary model.[27,28] The other models with $0 < \Lambda < \Lambda_2$ will also possess similar narrow regions corresponding to inflationary behavior, although of course there is no realistic late-time behavior in these cases. Despite the fact that the models we have considered do not describe physically realistic universes I hope that the analysis presented here will be useful for an overall understanding of the compactification process.

ACKNOWLEDGMENTS

I wish to thank Gary Gibbons for helpful discussions. This work was supported by an Isaac Newton grant.

[1]P. G. O. Freund and M. A. Rubin, Phys. Lett. **97B**, 233 (1980).
[2]P. Candelas and S. Weinberg, Nucl. Phys. **B237**, 397 (1984).
[3]Q. Shafi and C. Wetterich, Phys. Lett. **129B**, 387 (1983); **152B**, 51 (1985).
[4]P. G. O. Freund, Nucl. Phys. **B209**, 146 (1982).
[5]See E. W. Kolb, Fermilab Report No. 86-138-A, 1986 (unpublished), for a recent review. An extensive list of references is also given in K. Maeda, Class. Quantum Gravit. **3**, 233 (1986); **3**, 651 (1986).
[6]R. A. Matzner and A. Mezzacappa, Phys. Rev. D **32**, 3114 (1985).
[7]R. A. Matzner and A. Mezzacappa, Found. Phys. **16**, 227 (1986).
[8]G. W. Gibbons and P. K. Townsend, Nucl. Phys. **B282**, 625 (1987).
[9]V. A. Belinsky, L. P. Grishchuk, I. M. Khalatnikov, and Ya. B. Zeldovich, Phys. Lett. **155B**, 323 (1985); Zh. Eksp. Teor. Fiz. **89**, 346 (1985) [Sov. Phys. JETP **62**, 195 (1985)].
[10]G. W. Gibbons and D. L. Wiltshire, Nucl. Phys. **B287**, 717 (1987).
[11]F. R. Tangherlini, Nuovo Cimento **27**, 636 (1963).
[12]B. Carter, in *Black Holes,* Les Houches, 1972, edited by C. DeWitt and B. S. DeWitt (Gordon and Breach, New York, 1973).
[13]M. Simpson and R. Penrose, Int. J. Theor. Phys. **7**, 183 (1973).
[14]J. M. McNamara, Proc. R. Soc. London **A358**, 499 (1978); **A364**, 121 (1978).
[15]S. Chandrasekhar and J. B. Hartle, Proc. R. Soc. London **A384**, 301 (1982).
[16]H. Ishihara, Prog. Theor. Phys. **72**, 376 (1984).
[17]A. Chodos and S. Detweiler, Phys. Rev. D **21**, 2167 (1980).
[18]L. Brand, *Differential and Difference Equations* (Wiley, New York, 1966), p. 88.
[19]H. Sato, Prog. Theor. Phys. **72**, 98 (1984).
[20]D. Sahdev, Phys. Lett. **137B**, 155 (1984); Phys. Rev. D **30**, 2495 (1984).
[21]R. B. Abbott, S. M. Barr, and S. D. Ellis, Phys. Rev. D **30**, 720 (1984).
[22]E. W. Kolb, D. Lindley, and D. Seckel, Phys. Rev. D **30**, 1205 (1984).
[23]T. Koikawa and K. Maeda, Phys. Lett. **149B**, 82 (1984).
[24]K. Maeda, Phys. Rev. D **32**, 2528 (1985).
[25]Y. Hashimoto, Prog. Theor. Phys. **73**, 456 (1985).
[26]One can of course retain the equations we have studied and reverse the roles of the physical and internal spaces if the Freund-Rubin field is replaced by its dual $F = qa^m/b^n dt \wedge dx^1 \wedge \cdots \wedge dx^m$, similarly to (2.1). One would then need to study the solutions with n odd to obtain physically relevant results.
[27]Y. Okada, Phys. Lett. **150B**, 103 (1985).
[28]Y. Okada, Nucl. Phys. **B264**, 197 (1986).
[29]P. Forgács and Z. Horváth, Gen. Relativ. Gravit. **11**, 205 (1979).
[30]H. Nishino and E. Sezgin, Phys. Lett. **144B**, 187 (1984).
[31]A. Salam and E. Sezgin, Phys. Lett. **147B**, 47 (1984).
[32]K. Maeda and H. Nishino, Phys. Lett. **154B**, 358 (1985).
[33]K. Maeda and H. Nishino, Phys. Lett. **158B**, 381 (1985).
[34]S. R. Lonsdale, Phys. Lett. **175B**, 312 (1986).
[35]J. J. Halliwell, Nucl. Phys. **B286**, 729 (1987).
[36]J. J. Halliwell, Phys. Lett. **185B**, 341 (1987).
[37]J. B. Hartle and S. W. Hawking, Phys. Rev. D **28**, 2960 (1983).
[38]J. J. Halliwell, Nucl. Phys. **B266**, 228 (1986).